

**On a Method of Identification of Leptoquarks  
Produced in  $ep$  Collisions.**

V. Ilyin, A. Pukhov, V. Savrin, A. Semenov,  
*Institute of Nuclear Physics of Moscow State University, 119899 Moscow, Russia*  
and  
W. von Schlippe  
*Queen Mary & Westfield College, London, England*

**Abstract**

We analyse numerically manifestations of the radiative amplitude zero (RAZ) effect in single leptoquark production associated with hard photon emission. We present some quantitative conclusions on the possibility to distinguish leptoquark charges produced in  $ep$  collisions taking account of three-body final state subprocesses and of proton structure functions. Applying this method to HERA and possible LEP+LHC experiments we show that the RAZ analysis can serve as a tool to determine the leptoquark electric charge up to large leptoquark masses.

# 1 Introduction.

In paper [1] we have proposed a method for distinguishing the charges of leptoquarks<sup>1</sup> (LQ) produced in the reaction

$$e^\pm + p \rightarrow \gamma + LQ + X.$$

The idea is based on the radiative amplitude zero (RAZ) effect, i.e. the absence of photon emission at some directions depending on the leptoquark electric charges. In this paper we give a detailed numerical analysis of this method applying it to HERA and possible LEP+LHC experiments.

In Ref. [1] we have derived the analytical formulas for the unpolarized cross sections of the hard subprocesses

$$e^\pm + q \rightarrow \gamma + LQ \tag{1}$$

We have shown that they are proportional<sup>2</sup> to a factor  $(Q_e u - Q_q t)^2$ . So, at some photon emission angles where this factor vanishes the cross sections have exact zeros whose positions are completely determined by the electron (positron) and quark charges,  $Q_e$  and  $Q_q$ , respectively.

Of course in reality the leptoquarks decay into two fermions. Considering the electron decay channel we have got the following clear signature: the hard photon, the electron (or positron) and a hard (quark) jet with complete kinematical reconstruction of the subprocess:

$$e^\pm + q \rightarrow \gamma + e^\pm + q \tag{2}$$

In this paper we analyse numerically the manifestations of the RAZ effect for the case of this three-body final state subprocess. We make some quantitative conclusions on a possibility to distinguish the charges of leptoquarks produced in  $ep$  collisions taking account of the proton structure functions.

Our calculations were made with the help of the CompHEP package [3] created for automatic calculation of cross sections at tree level in the Standard Model and beyond. For the numerical integration over three-particle phase space and for event generation we have used the BASES package [4].

## 2 Calculation framework

The amplitude of subprocess  $e^- + d \rightarrow e^- + d + \gamma$  is represented by the Feynman diagrams displayed in Figs. 1, 2. In Fig. 1 the diagrams corresponding to the signal LQ production process (2) are represented. The diagrams of Fig. 2 correspond to the SM contribution: deep inelastic scattering associated with hard photon emission.

Using the CompHEP package we have calculated analytically the unpolarized squared matrix elements for subprocesses (2). But in contrast to our previous paper [1] we have introduced finite widths into the LQ propagators. Then we have evaluated numerically the contribution of separate (quark) constituents to the integrated cross sections by the convolution of the subprocess cross section with the corresponding parton distribution function:

$$\sigma(s) = \int_{x_{min}}^1 dx q(x, Q^2) \int d\Phi_3 \frac{d\hat{\sigma}}{d\Phi_3} \Theta_{cuts}(E_\gamma, \vartheta_\gamma, \dots). \tag{3}$$

Here  $d\Phi_3$  is the element of 3-body phase space;  $\hat{\sigma}$  is the cross section of subprocess (2);  $s$  is the squared CMS energy of the electron-proton system; the squared CMS energy of the hard subprocess equals  $\hat{s} = xs$ ; the quark distribution function is denoted by  $q(x, Q^2)$  and the 4-momentum transfer scale is taken to be  $Q = \sqrt{\hat{s}}$ . The photon emission angle is denoted by  $\vartheta_\gamma$ . The direction  $\vartheta_\gamma = 0$  is along the proton beam. As the lower bound  $x_{min}$  we use the value  $M^2/s$  to take into account the quasi-resonant peak, where  $M$  is the LQ mass. The function  $\Theta_{cuts}(E_\gamma, \vartheta_\gamma, \dots)$  corresponds to the kinematical cuts which we impose to get a realistic distribution and values of cross sections. In particular this function has to include cuts on the photon energy and on the angles between the photon and all charged particles in (2) to remove infrared and collinear divergences. It is also necessary to apply cuts for a reliable separation of the hard jet.

---

<sup>1</sup>The problem of identification of LQ is discussed now in the literature, see recent publication [2] where the determination of the leptoquark properties in polarized  $e\gamma$  collisions is considered.

<sup>2</sup>For the vector leptoquark this is correct only in the case of Yang-Mills coupling.

All the fermion masses are put equal to zero in our calculations.

The numerical analysis of the corresponding cross sections is given for two cases:

- HERA:  $\sqrt{s} = 296$  GeV, electron beam energy  $\mathcal{E}_e = 26.7$  GeV, integrated luminosity  $L = 100$  pb $^{-1}$ ;
- LEP+LHC:  $\sqrt{s} = 1740$  GeV,  $\mathcal{E}_e = 100$  GeV, annual integrated luminosity  $L = 1000$  pb $^{-1}$ .

One of the general restrictions on the LQ-fermion interaction is the chirality of the fermion-LQ coupling (see [5] and references therein). Therefore we consider only either couplings with left-handed leptons or with right-handed ones. In both cases we use in the numerical analysis an “electroweak” value for this constant,  $\lambda = 0.3$ .

As to LQ mass we analyse cross sections in the following ranges

- HERA:  $150 \text{ GeV} < M < 290 \text{ GeV}$ ;
- LEP+LHC:  $200 \text{ GeV} < M < 1500 \text{ GeV}$ .

For the parton densities we used the parametrizations STEQ2p [6] and MRS-A [7], which take account of recent HERA data. Both parametrizations gave the same results within calculation error.

Let us describe in more detail the cuts which we apply in the laboratory frame.

For a proper background analysis we introduce kinematical cuts for this reaction in such a way as to suppress contributions from the Standard Model Feynman diagrams (see Fig. 2). Recall that for the problem under consideration the LQ mass is supposed to be already known from resonant LQ production. So we can introduce a narrow cut on the invariant mass of the outgoing electron (or positron) and the (quark) jet:

$$|(p_e^{out} + p_q^{out})^2 - M^2| < 6M\Gamma, \quad (4)$$

where  $\Gamma$  is the LQ width. We have calculated  $\Gamma$  at tree level for each value of the LQ mass.

We introduce also a cut on the angle between the outgoing electron (positron) and the quark:  $\vartheta_{eq} > 10^\circ$ . In the case of LQ decay the products are moving back-to-back in the LQ rest frame, so this cut suppresses the standard model contributions and does not change the LQ signal.

Then we have to introduce cuts on the energies and emission angles of the outgoing electron (positron) and quark to exclude the forward and backward cones and various soft contributions:

$$E_e, E_q > 10 \text{ GeV}, \quad 10^\circ < \vartheta_e, \vartheta_q < 170^\circ. \quad (5)$$

We also apply cuts on the photon energy and emission angle:  $E_\gamma > 1$  GeV,  $10^\circ < \vartheta_\gamma < 170^\circ$ .

Finally we introduce cuts on the angles between the outgoing photon and the electron (positron) and quark:  $\vartheta_{\gamma e} > 10^\circ$ ,  $\vartheta_{\gamma q} > 10^\circ$ . These cuts remove the collinear divergences.

For this set of cuts and with  $x_{min} = (200 \text{ GeV})^2/s$  the cross sections of reaction (2) calculated in the Standard Model are:

$$\begin{array}{ll} \text{HERA} & \sigma_{\text{SM}} \sim 0.5 \text{ fb;} \\ \text{LEP+LHC} & \sigma_{\text{SM}} \sim 40 \text{ fb.} \end{array}$$

So, for our analysis we have an SM background of less than 1 event for HERA (assuming an integrated luminosity of 100 pb $^{-1}$ ) and less than 50 events per year for LEP+LHC. For larger LQ masses from the corresponding ranges (see above) we introduce larger cuts  $x_{min}$ , so the SM background is smaller.

The final results presented in this paper were calculated for reaction (2) with a complete set of tree level diagrams, i.e. taking into account the SM diagrams, the contributions of the signal reaction (1) and the SM-LQ interference terms.

### 3 Numerical results and RAZ analysis

In this section we present results of the numerical analysis for the left-handed sector of LQ-fermion interactions. For the right-handed sector the results for all channels are the same as for the corresponding processes in the left-handed sector due to identical analytical formulæ [1]. For the leptoquarks we use the notation of [5] (see also the detailed table of LQ quantum numbers in [1]).

First we note that the cross sections of interest are of order 1 pb for HERA and 10 pb for LEP+LHC. These values are obtained for reaction (2) with the kinematical cuts discussed in section 2 and with

$M = 200$  GeV for HERA and  $M = 300$  GeV for LEP+LHC with an electroweak value of the fermion-LQ coupling constant  $\lambda = 0.3$ . So, there are about one-hundred events at HERA and more than ten thousand events at LEP+LHC. This must be compared with the SM background, which is less than 1 event at HERA and 50 events per year at LEP+LHC.

A typical example of a distribution in  $x$  is shown in Fig. 3, for the  $S_3^{-1}$  leptoquark with  $\sigma = 0.82$  pb for HERA at  $M = 200$  GeV and  $\sigma = 13$  pb for LEP+LHC at  $M = 300$  GeV. One can see that there is a sharp peak near  $x_{min} = M^2/s$ .

The cross sections decrease with increasing leptoquark mass. This is shown in Fig. 4 for HERA and in Fig. 5 for LEP+LHC.

In Fig. 6 we present the angular distributions of hard photons for the case of scalar leptoquarks and  $u$  and  $d$  valence quarks. Again we present these distributions at  $M_{LQ} = 200$  GeV for HERA and at  $M_{LQ} = 300$  GeV for LEP+LHC.

For HERA we took 16 bins,  $10^\circ$  per bin. Due to the small statistics (even for an integrated luminosity of  $100 \text{ pb}^{-1}$ ) a finer binning does not allow us to recognize the RAZ effect. For LEP+LHC we took 40 bins,  $4^\circ$  per bin. We see explicit RAZ for  $S_3^{-1}$  and  $R_2^{-\frac{1}{2}}$  leptoquarks at different values of RAZ angles in good agreement with Ref. [1] where the RAZ angles were estimated analytically. For the  $e^-u$  channel (leptoquarks  $S_1, S_3^0$ ) this angular distribution has no radiative amplitude zero<sup>3</sup> and the distribution in the  $e^+d$  case is similar.

The angular distributions in  $\vartheta_\gamma$  for vector leptoquarks with Yang-Mills couplings and valence quarks in the initial state have a behaviour similar to the corresponding cases for scalar LQ; they are therefore not shown.

Also for channels with sea quarks the distributions in the photon emission angle are similar but with a significantly smaller level of cross sections (see Fig. 5). Note that for HERA there is no statistics for any of the processes in the channels with sea quarks.

Considering these distributions we see that for HERA the RAZ analysis seems to be statistically unsupported in the case of leptoquark masses greater than 200 GeV (for  $\lambda = 0.3$ ). However from the HERA data analysis corresponding to an integrated luminosity of  $\approx 425 \text{ nb}^{-1}$  [8] for the  $R_2$  and  $\tilde{R}_2$  scalar LQ and for the  $U_1, \tilde{U}_1$  and  $U_3$  vector LQ the established mass limit is smaller than 200 GeV (for  $\lambda = 0.3$ ). In this small mass range between the experimental limit and 200 GeV the determination of the LQ electric charge is still possible by the proposed method if this new boson is discovered at HERA.

For LEP+LHC there is enough statistics for a reliable RAZ analysis up to large leptoquark masses. Consider, as a criterion, 10 events per  $4^\circ$  bin, in which case we can say with confidence whether RAZ is present or absent. There are 40 bins in the interval  $10^\circ < \vartheta_\gamma < 170^\circ$ , so the lower limit for the cross section is 0.4 pb to be certain that RAZ is statistically visible. From the leptoquark mass dependence of the cross sections (see Fig. 4 and Fig. 5) we derive the upper limits for leptoquark masses with visible RAZ. These mass limits are shown in Table 1.

We see that for LEP+LHC the RAZ analysis, and indeed a measurement of the leptoquark charge, can be made in the  $e^-p$  and  $e^+p$  channels separately up to  $M \sim 500 - 600$  GeV for all types of leptoquarks. For higher masses, up to 850 – 900 GeV, all types of leptoquarks could also be identified but only some of them in the  $e^-p$  channel and others in the  $e^+p$  channel. The upper limit for the RAZ analysis is about  $M \sim 1$  TeV, see details in Table 1. For the vector case the situation is slightly better for  $U_3$  and  $\tilde{U}_1$  leptoquarks. Here the RAZ effect can be reliably determined up to  $M \sim 1200$  GeV.

Note that the pairs  $(S_1, S_3^0)$  and  $(U_1, U_3^0)$  (in the left-handed sector) will remain unresolved by this method, because of their equal charges and third components of isospin.

Finally we note that our analysis was made for the reaction with the electron decay mode of LQ. So only leptoquarks with the third components of isospin equal to  $-1$  and  $-\frac{1}{2}$  from the corresponding isotriplets and isodoublets were considered in the analysis (with the only exception of  $R_2$  and  $V_2$  in the right-handed sector). To analyse leptoquarks with complementary isospin projections from the same multiplet it is necessary to investigate the neutrino decay mode of LQ. However the signature of these processes includes missing energy due to the neutrino emission. So one has to carry out the analysis differently in this case. This analysis will be presented elsewhere.

---

<sup>3</sup>The drop in the bin  $130^\circ < \vartheta_\gamma < 140^\circ$  in this channel is a statistical fluctuation.

# Conclusions

Our principal conclusion is that for some types of leptoquarks (in the left-handed sector:  $S_3^{-1}$  and  $R_2^{-\frac{1}{2}}$  scalars,  $V_2^{-\frac{1}{2}}$  and  $U_3^{-1}$  vectors; in the right-handed sector:  $\tilde{S}_1$  and  $R_2^{-\frac{1}{2}}$  scalars,  $V_2^{-\frac{1}{2}}$  and  $\tilde{U}_1$  vectors) the *radiative amplitude zero* is present in the distribution in the photon emission angle. This effect can be detected at LEP+LHC up to large values of leptoquark masses: 900 GeV for  $S_3^{-1}$  and  $V_2^{-\frac{1}{2}}$ , 1 TeV for  $R_2^{-\frac{1}{2}}$  and 1.2 TeV for  $U_3^{-1}$  and  $\tilde{U}_1$ .

The RAZ analysis (whether the radiative amplitude zero is present or not) gives us a possibility to determine the leptoquark electric charge (and, as a result, its other quantum numbers). This method is available up to rather large leptoquark masses (up to 1 TeV at LEP+LHC). Even at HERA there still exists a small mass region (near 200 GeV) for some leptoquarks where the RAZ effect can be observed.

For vector leptoquarks the exact RAZ effect is present only in the case of Yang-Mills type of photon-LQ coupling. So we have got a fairly sensitive tool to measure the anomalous magnetic moment  $\kappa$  in the case of RAZ. A detailed analysis of this possibility will be presented in a future publication.

All our numerical results were obtained for the electroweak value of the fermion-LQ coupling constant,  $\lambda = 0.3$ . For other values of  $\lambda$  numerical estimates can be obtained by rescaling our results (cross sections have  $\lambda^2$  as a factor).

# Acknowledgements

This work was partly supported by the Royal Society of London as a joint project between Queen Mary & Westfield College (London) and Institute of Nuclear Physics, Moscow State University, and by INTAS (project 93-1180). V.I. and V.S. wish to thank QMW for their hospitality and the possibility to work during their visit in London. WvS wishes to thank INP-MSU for hospitality. The work of V.I., A.P. and A.S. was partly supported by Grants M9B000 and M9B300 from the International Science Foundation.

# References

- [1] V.A. Ilyin et al., INP MSU Preprint-95-1/365, QMW-PH-95-6, 1995; hep-ph/9503401; Phys. Lett. B (to be published).
- [2] M.A. Doncheski and S. Godfrey, Phys. Rev. **D51** (1995) 1040.
- [3] E. Boos et al., INP MSU-94-36/358, SNUTP 94-116, Seoul. 1994; hep-ph/9503280.
- [4] S. Kawabata, Comp. Phys. Comm. **41** (1986) 127.
- [5] W. Buchmüller, R. Rückl and D. Wyler, Phys. Lett. **B191** (1987) 442.
- [6] J. Botts et al. (CTEQ Collaboration), Phys. Lett. **B304** (1993) 159; H.L. Lai et al. (CTEQ Collaboration), Michigan State University preprint MSU-HEP-41024 (1994).
- [7] A.D. Martin, R.G. Roberts and W.J. Stirling, Phys. Rev. **D50** (1994) 6734.
- [8] H1 Collaboration, T. Ahmed et al., Z. Phys. C64 (1994) 545. ZEUS Collaboration, M. Derrick et al., Phys. Lett. **B306** (1993) 173.

# Table

# Figures captions

Figure 1: Feynman diagrams with LQ signal.

Figure 2: Feynman diagrams for subprocesses  $e^- + q \rightarrow e^- + q + \gamma$  in SM.

Figure 3: Distributions in  $x$  for  $e^- + d \rightarrow \gamma + e^- + d$  with the  $S_3^{-1}$  leptoquark contribution. These distributions are obtained at  $M = 200 \text{ GeV}$  for HERA ( $\sigma = 0.82 \text{ pb}$ ) and at  $M = 300 \text{ GeV}$  for LEP+LHC ( $\sigma = 13 \text{ pb}$ ) with kinematical cuts applied.

Figure 4: Cross sections in dependence on the LQ mass at HERA.

Figure 5: Cross sections in dependence on the LQ mass at LEP+LHC.

Figure 6: Distributions in the photon emission angle  $\vartheta_\gamma$  for valence quarks ( $M = 200 \text{ GeV}$  for HERA and  $M = 300 \text{ GeV}$  for LEP+LHC) in the case of scalar LQ.

$\ell q$ channel		$e^-u$	$e^-d$	$e^-\bar{u}$	$e^-\bar{d}$	$e^+u$	$e^+d$	$e^+\bar{u}$	$e^+\bar{d}$
scalar LQ	L	$S_1, S_3^0$	$S_3^{-1}$	$R_2^{-\frac{1}{2}}$	$\tilde{R}_2^{-\frac{1}{2}}$	$R_2^{-\frac{1}{2}}$	$\tilde{R}_2^{-\frac{1}{2}}$	$S_1, S_3^0$	$S_3^{-1}$
	R	$S_1$	$\tilde{S}_1$	$R_2^{-\frac{1}{2}}$	$R_2^{\frac{1}{2}}$	$R_2^{-\frac{1}{2}}$	$R_2^{\frac{1}{2}}$	$S_1$	$\tilde{S}_1$
max $M$ [GeV]		900	900	540	610	980	830	670	500
vector LQ	L	$\tilde{V}_2^{-\frac{1}{2}}$	$V_2^{-\frac{1}{2}}$	$U_3^{-1}$	$U_1, U_3^0$	$U_3^{-1}$	$U_1, U_3^0$	$\tilde{V}_2^{-\frac{1}{2}}$	$V_2^{-\frac{1}{2}}$
	R	$V_2^{\frac{1}{2}}$	$V_2^{-\frac{1}{2}}$	$\tilde{U}_1$	$U_1$	$\tilde{U}_1$	$U_1$	$V_2^{\frac{1}{2}}$	$V_2^{-\frac{1}{2}}$
max $M$ [GeV]		1140	910	610	690	1180	830	660	660

Table 1: LEP+LHC. The RAZ upper limits for LQ masses (in the positron channels anti-LQ are produced). L-row corresponds to the interaction of LQ with left-handed leptons and R-row to right-handed ones.

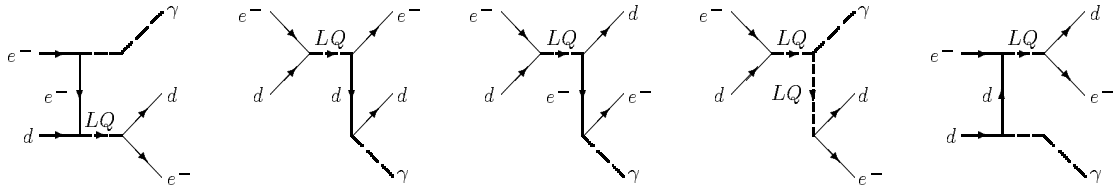


Figure 1:

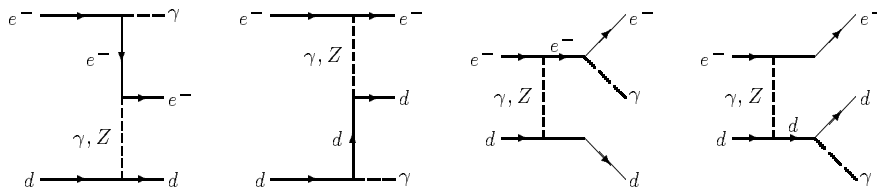


Figure 2:

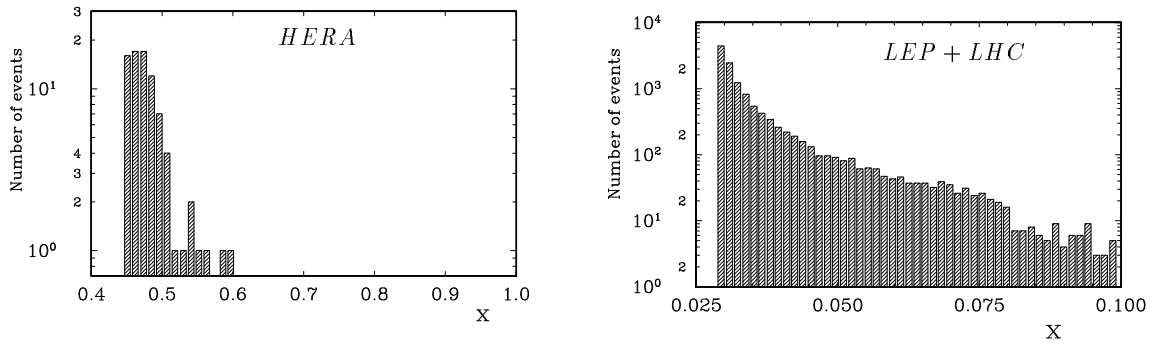


Figure 3:

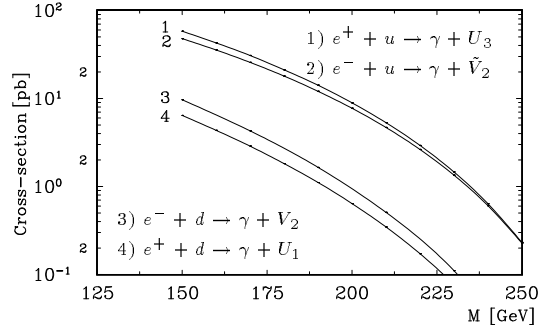
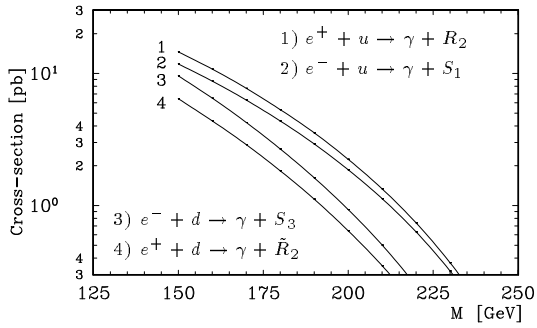


Figure 4:

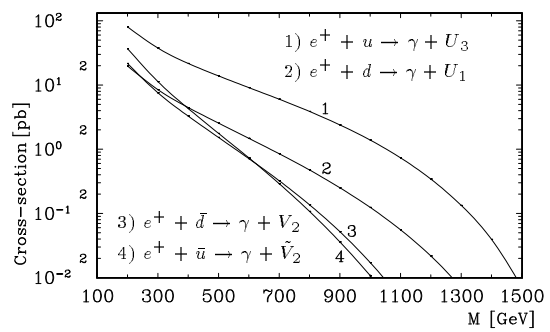
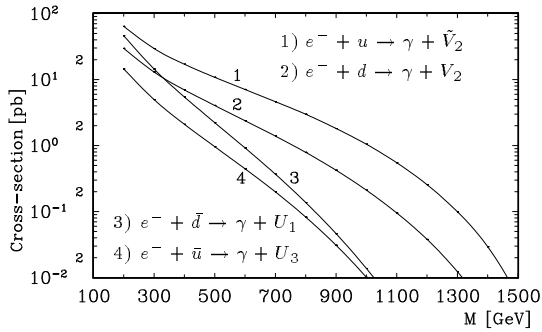
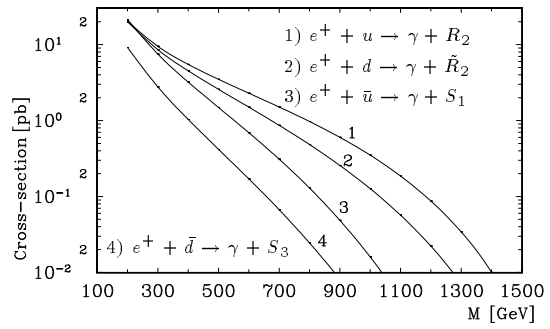
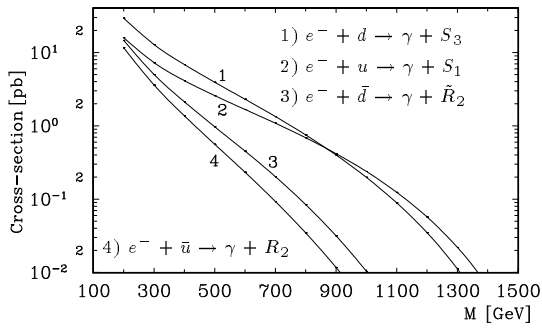


Figure 5:

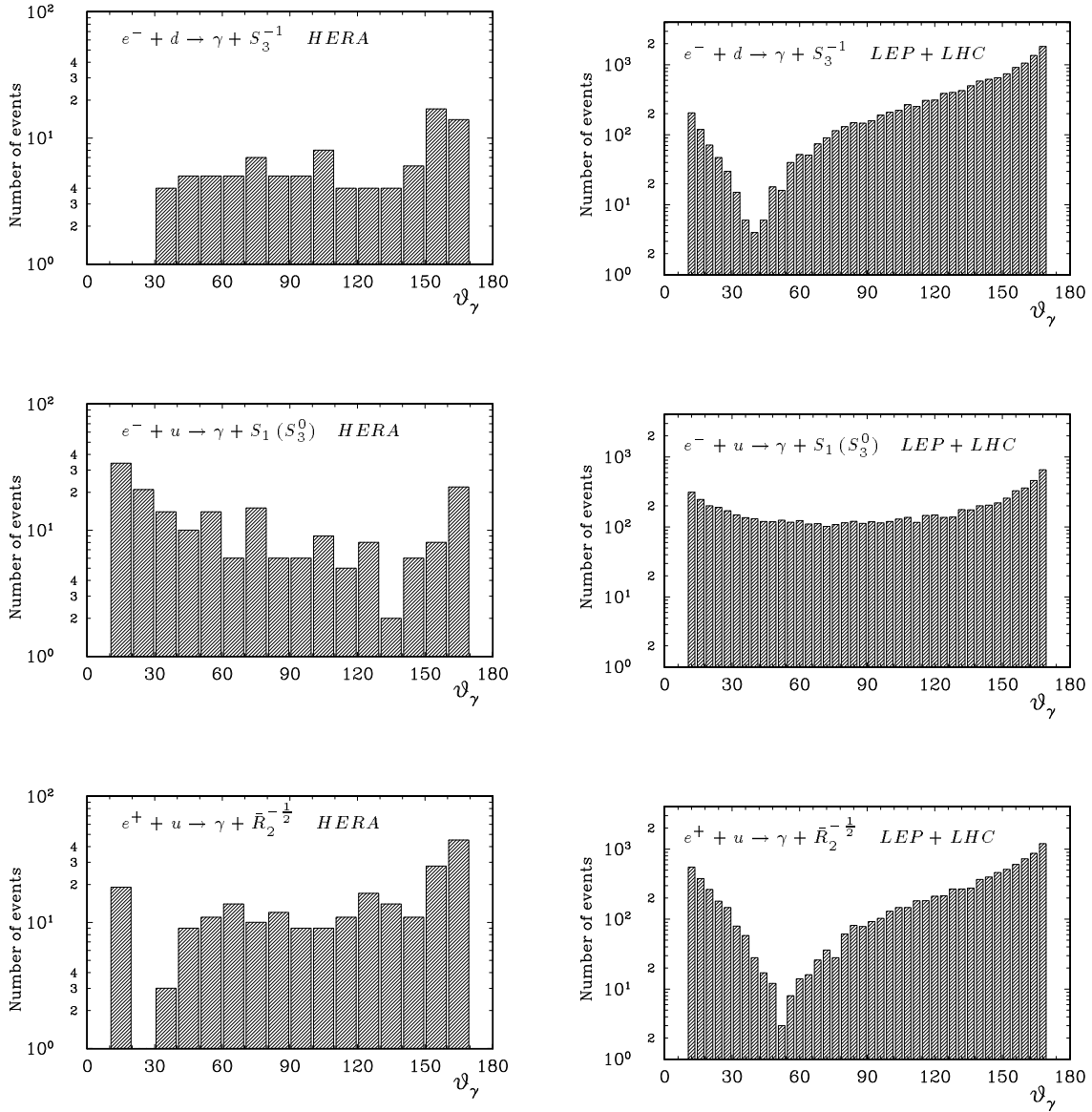


Figure 6: